Rapid #: -26125423

CROSS REF ID: **789908**

LENDER: **CBA (California State Univ Bakersfield) :: Main Library**

BORROWER: **MYG (MIT (Massachusetts Inst. of Technology)) :: Main Library**

TYPE:	Article CC:CCG
JOURNAL TITLE:	Separation and purification technology
USER JOURNAL TITLE:	Separation and Purification Technology
ARTICLE TITLE:	Continuous purification of mRNA by precipitation and sequential TFF
ARTICLE AUTHOR:	Pons Royo
VOLUME:	379
ISSUE:	
MONTH:	
YEAR:	2025
PAGES:	134837-
ISSN:	1383-5866
OCLC #:	

Processed by RapidX: 2/9/2026 5:03:47 PM

Separation and Purification Technology 379 (2025) 134837

Contents lists available at ScienceDirect

Separation and Purification Technology

journal homepage: www.elsevier.com/locate/seppur

Continuous purification of mRNA by precipitation and sequential TFF

Maria del Carme Pons Royo [a], Tyler Arnold [a], Isabella Perez Rodriguez [a], Nicole Ostrovsky [b,c], Mushriq Al-Jazrawe [b,c], Andrew Hatas [a], Allan S. Myerson [a], Richard D. Braatz [a,*]

[a] Department of Chemical Engineering, Massachusetts Institute of Technology, 77 Massachusetts Avenue, Cambridge, MA 02139, The United States of America
[b] Koch Institute for Integrative Cancer Research, Massachusetts Institute of Technology, Cambridge, MA, The United States of America
[c] Broad Institute of MIT and Harvard, Cambridge, MA, The United States of America

ARTICLE INFO

Editor:Raquel Aires Barros

Keywords:
Precipitation
mRNA
Vaccines
Purification
Downstream processing
Bioprocess development
Continuous

ABSTRACT

Since the clinical trials for the first COVID-19 vaccines in 2020, interest in RNA-based therapeutics has grown rapidly, with promising applications in vaccines, oncology, and gene therapy. This surge has created a strong demand for scalable, cost-effective, and robust manufacturing platforms for messenger RNA. However, current mRNA purification largely relies on batch-wise chromatography and tangential flow filtration, which face limitations in scalability, cost, and compatibility with continuous production. Chromatographic techniques often require harsh conditions, such as high pH, salt, or organic solvents, that may compromise mRNA stability. Additionally, extensive sample conditioning (e.g., dilution, heating) is typically required to reduce aggregation and facilitate column loading, further hindering continuous operation. To address these challenges, a fully continuous precipitation-based method for mRNA purification is developed. The process consists of an optimized precipitation step using PEG6000 and NaCl in a tubular reactor, followed by two continuous TFF stages for washing and buffer exchange. The overall process achieves yields of 92 % and purities of 95 %, with no detectable double-stranded RNA formation, residual proteins, fragmentation, or aggregates. Compared to traditional approaches, this method achieves higher yields and purities while offering enhanced process robustness and integration potential. The final mRNA product can be directly encapsulated into lipid nanoparticles without further conditioning, with no observed degradation or aggregation. This platform offers a scalable, flexible alternative to chromatography, suitable for integration into end-to-end continuous mRNA manufacturing.

1. Introduction

Since the launch of clinical trials for the first COVID-19 vaccines in 2020, interest in RNA-based therapeutics has grown rapidly [1,2]. These technologies hold promise across a wide range of applications, including vaccines, cancer treatments, and gene therapies [3]. As a result, the demand for messenger RNA (mRNA) manufacturing has increased significantly, highlighting the need for scalable and efficient production methods, along with reliable analytical techniques to ensure consistent product quality, safety, and efficacy [4,5]. However, meeting this demand remains challenging, as current mRNA purification processes still rely on traditional methods such as tangential flow filtration (TFF) and chromatography, which often present limitations in terms of scalability and cost-effectiveness [6]. While various chromatographic techniques have been applied to mRNA purification, each presents its own set of limitations [7]. For instance, anion-exchange chromatography requires high pH [8], hydrophobic interaction chromatography uses high salt concentrations in buffers [9], and reverse-phase chromatography involves the use of organic solvents [10,11]. These harsh conditions can compromise mRNA integrity [7]. Additionally, the complex secondary structure of mRNA, particularly in transcripts longer than 500 nucleotides, makes it prone to aggregation [12]. To enhance resolution and increase binding capacity in purification methods such as Oligo dT affinity chromatography [13–17] or anion exchange chromatography [18], these structures must be disrupted. Before downstream processing, crude in vitro transcription (IVT) products must be diluted up to 50-fold and incubated at 70 °C for several minutes. These preparatory steps, which also include buffer exchange and preheating, are necessary to

* Corresponding author.
E-mail addresses: ponsroyo@mit.edu (M.C. Pons Royo), braatz@mit.edu (R.D. Braatz).

https://doi.org/10.1016/j.seppur.2025.134837
Received 8 July 2025; Received in revised form 16 August 2025; Accepted 19 August 2025
Available online 20 August 2025

solubilize the mRNA, improve filtration efficiency, and prevent clogging during chromatographic purification. However, such extensive conditioning hinders the implementation of continuous processing, limiting scalability and contributing to higher production costs and lower yields. This highlights the need for a more flexible, cost-effective downstream purification strategy.

To overcome these limitations and enable continuous, scalable purification, alternative strategies are being explored. Among them, precipitation has emerged as a promising solution [19–28]. This method is favored not only for its low cost and flexibility but also for its ease of adaptation to continuous processes and scalability. Over the past decade, precipitation and filtration techniques have been explored for capturing recombinant antibodies. Continuous precipitation can be achieved using tubular reactors equipped with static mixers, followed by washing the precipitates with a series of filters. Furthermore, precipitation has been found to be particularly effective for high-titer applications, offering a more cost-efficient alternative to affinity chromatography. mRNA has been demonstrated to precipitate efficiently at room temperature using a combination of NaCl and polyethylene glycol (PEG). Precipitation occurs mainly due to the addition of cations, which neutralize the negative phosphate backbone of the mRNA. PEG enhances precipitation selectivity by reducing the required cation concentration, preventing co-precipitation, and selectively precipitating larger molecules while allowing smaller impurities to remain in solution.

Herein, we present a feasibility study for the purification of mRNA from IVT crude using a continuous precipitation process. The method comprises two stages: an initial precipitation step utilizing PEG 6000 and NaCl, previously optimized in a tubular reactor, followed by two continuous tangential flow filtration steps (TFF) for washing and impurity removal and buffer exchange. The results obtained from continuous operation are compared to those obtained from a comparable batch operation. This purification method can be directly integrated into any mRNA production process.

2. Materials and methods

2.1. mRNA pure and crude constructs

Experiments were performed with different mRNA samples from crude IVT solution provided by Arranta Bio (Recipharm AB, USA), previously used in Pons Royo et al. [29] mRNA samples were stored at − 20 °C for short-term storage and at − 80 °C for long-term storage.

2.2. Reagents

Unless otherwise noted, analytical-grade reagents were used throughout the study and sourced from Sigma-Aldrich (St. Louis, MO, USA) or MilliporeSigma (Burlington, USA). Solutions were prepared using RNAse-free water from the Direct-Q® 3 Remote Kit with a Biopak Final Filter, and Nuclease & Endotoxin-Free Water from MilliporeSigma (Burlington, USA).

2.3. pH screenings

For the pH precipitation screenings, 100 μL of crude IVT mRNA solution was precipitated using 2.5 M sodium chloride stock solution and 40 % PEG6000 were added to 100 μL of crude IVT mRNA solution to achieve final concentrations of 250 sodium chloride and 5, 7, 9, 11, 13, and 15 % PEG in different buffers (100 mM citrate buffer pH 4, 100 mM sodium citrate buffer pH 5.6, 100 mM MES buffer pH 7, 100 mM Tris buffer pH 8 and pH 9) in 96 well plates. The 96 well plates were incubated on a microplate shaker at 500 rpm for 60 min. After incubation, the 96 well plates were centrifuged (Eppendorf Centrifuge 5425 R) at 2,000 rpm for 15 min. The supernatant was discarded, and the precipitates were resuspended in 100 μL RNAse free water. Yield and purity were evaluated using size exclusion chromatography [29].

2.4. Temperature screenings

For the temperature screenings, 100 μL of crude IVT mRNA solution was precipitated using 2.5 M sodium chloride stock solution and 40 % PEG6000 to achieve final concentration of 250 mM sodium chloride and 13 % PEG. Precipitation screening experiments were conducted in 2 mL Eppendorf tubes by combining predetermined volumes of the respective precipitating solutions. Samples were then mixed on an end-over-end rotator at 20 rpm for 1 h to allow precipitation to occur. After incubation, the tubes were centrifuged (Eppendorf Centrifuge 5425 R) at 12,000 rpm for 15 min. The supernatant was collected for further analysis, while the pellet was resuspended in 0.5 mL of RNase-free water. Afterwards, Eppendorf tubes were incubated in a water bath at different temperatures (40 °C, 50 °C, 60 °C, and 70 °C) for 2, 5, and 10 min to assess the impact of heat on HMWI reduction. 100 μL sample were taken and analysed by size exclusion chromatography.

2.5. Critical flux and filtration module determination

Critical flux experiments were conducted as previously described [30] using various hollow fiber membranes. Initial trials involved evaluating different membrane materials, mixed esters (ME) and polyethersulfone (PES), followed by testing hollow fibers with different inner diameters (0.5 mm and 1 mm). A precipitate suspension was prepared by mixing Fluc mRNA with 40 % (w/w) PEG6000 and 0.8 M NaCl, and then introduced into the system using a peristaltic pump (KrosFlo Research Jr, Repligen, Waltham, USA) at a flow rate of 50 mL/min. The feed solution was drawn from a 50 mL Falcon tube and directed to the filter inlet, with both retentate and permeate recirculated back into the same reservoir. To regulate and adjust the permeate flux, a second peristaltic pump (KrosFlo Research Jr, Repligen, Waltham, USA) was employed, varying the flux within a range of 46 LMH to 231 LMH. Transmembrane pressure (TMP) was continuously monitored using pressure sensors (PendoTech, New Jersey, US) positioned at the inlet, retentate, and permeate lines of the hollow fiber membrane system and connected to the KRoFLos system. Subsequently, the precipitated mRNA was diluted to the working concentration using the washing buffer composed of 750 mM sodium acetate at pH 5.5 and then used to determine the critical flux during the second TFF step, applying the same flow conditions.

2.6. Continuous precipitation

A continuous precipitation process was established using a custom-assembled tubular reactor system. Standard laboratory tubing (Tygon® R-3603, inner diameter 3.20 mm; Avantor, USA) packed with static mixers (HT-40–3.18–12-AC, made of Acetal; Stamixco AG, New York, USA). The system was connected using Luer fittings (Cole-Parmer). The IVT crude was pumped continuously at 0.35 mL/min and combined with a feed stream of 0.15 mL/min containing 40 % (w/w) PEG6000 and 0.8 M NaCl. This mixing ratio established precipitation conditions of 13 % (w/w) PEG6000 and 250 mM NaCl [29]. Under these conditions, the tubular reactor provided a residence time of 20 min. Subsequently, the precipitate was transferred to the first TFF stage, where it was concentrated and washed using a solution containing 13 % (w/w) PEG6000 and 250 mM NaCl. This step was performed with a PES 0.2-μm hollow fiber module (Repligen) with a filtration area of 13 cm^2. In the second TFF stage, the precipitate was further washed and buffer exchanged with a solution containing 750 mM NaAc, utilizing the same type of hollow fiber module. Both filtration stages operated at a flow rate of 50 mL/min, with permeate flow rates of 2.5 mL/min in the first stage and 3 mL/min in the second. Additionally, two peristaltic pumps (Ismatec ISM 597; Cole-Parmer) operated at 0.5 mL/min to transfer the concentrated precipitate from the first to the second TFF stage and

subsequently to a junction. At this junction, an additional peristaltic pump (Ismatec ISM 597; Cole-Parmer) introduced water at a flow rate of 9.5 mL/min, after which the final solution was directed through a water bath (Ismatec ISM 597; Cole-Parmer) at 70 °C for 2 min.

2.7. Size exclusion chromatography (SEC)

An Agilent Bio SEC-5 column (2000Å, 4.6 × 150 mm, 5 μm) from Agilent (Santa Clara, CA, USA) was used for analysis. The mobile phase consisted of a 100 mM phosphate buffer at pH 7, maintained at an isocratic flow rate of 0.35 mL/min. Before use, the buffer was filtered through 0.22 μm filters (Merck KGaA, Darmstadt, Germany) and degassed. A sample volume of 1 μL was injected, and absorbance at 260 nm was recorded using a Vanquish HPLC system equipped with a diode array detector (Thermo Fisher Scientific, MA, USA). Data analysis was performed using Chromeleon™ software (Thermo Fisher Scientific, MA, USA). High molecular weight impurities (HMWI) were identified as peaks eluting before 8 min, while the main mRNA peak appeared between 8 and 9.5 min. Peaks eluting after 10 min were classified as low molecular weight impurities (LMWI). mRNA purity was determined by calculating the ratio of the mRNA peak area to the total peak area at 260 nm. The concentration of mRNA and impurities was estimated by integrating the total area in size-exclusion chromatography and comparing it to a calibration curve created using a known mRNA concentration [29].

2.8. dsRNA detection

Double-stranded RNA levels were measured using the Lumit® dsRNA Detection Assay (Promega, W2041), following the manufacturer's instructions. In short, serial dilutions of both samples and a dsRNA standard were mixed with the dsRNA Sensor Reagents. After adding the detection substrate, luminescence was recorded using a Varioskan Flash microplate reader (Thermo Scientific). dsRNA concentration was interpolated from standard curve and reported as a percentage of total mRNA, as previously in Pons Royo et al. [29].

2.9. Capillary gel electrophoresis (CGE)

Fragment analysis of mRNA samples was conducted using a 5200 Fragment Analyzer system (Agilent Technologies). RNA was analyzed on the Agilent Fragment Analyzer at standard sensitivity using RNA separation gel on protocol DNF-471–33, as previously in Pons Royo et al. [29].

2.10. Protein concentration

Protein levels were quantified using the Invitrogen Qubit™ Protein Assay Kit with fluorescence detection on a Tecan Infinite microplate reader, in accordance with the supplier's guidelines. Fluorescent signals from dye–protein complexes were detected with the same device, and concentrations were derived from calibration curves prepared using the RNA and protein standards included in the Qubit™ kits [29].

2.11. Cell culture transfection and luciferase assay

Lenti-X 293 T cells (Takara Bio, Cat. no. 632180) were cultured in Dulbecco's Modified Eagle's Medium (DMEM; Thermo Fisher Scientific, 11995073) supplemented with 10 % fetal bovine serum (Thermo Fisher Scientific, A5669801) and 1 × antibiotic–antimycotic (Thermo Fisher Scientific, 15240112). Cells were maintained at 37 °C in a humidified 5 % CO_2 incubator and passaged at ~ 80 % confluence using TrypLE Express (Thermo Fisher Scientific, 12604039), followed by centrifugation at 250 × g for 5 min and reseeding at a 1:3 split ratio. For transfection, cells were seeded in opaque white 96-well plates (Corning, 3917) at 10,000 cells per well in 250 μL of culture medium, 24 h prior to transfection. On the day of transfection, the medium was replaced with 200 μL of fresh medium. Transfections were carried out using Lipofectamine MessengerMAX (Thermo Fisher Scientific, LMRNA001) according to the manufacturer's instructions. Each well received 100 ng of mRNA (or the amount indicated in each figure) and 0.15 μL of Lipofectamine. For each mRNA sample, three independent mRNA–lipid complexes were prepared and each was added to three separate wells (nine wells per mRNA sample in total). One additional well received mRNA without Lipofectamine as a negative control. Cells were incubated for 24 h post-transfection before analysis. Luciferase activity was measured using the ONE-Glo EX Luciferase Assay System (Promega, E8110). At 24 h post-transfection, 100 μL of culture medium was removed and replaced with 100 μL of reconstituted luciferase reagent. Liquid handling was performed using the Integra Assist Plus system (Integra Biosciences, Hudson, NH, USA). Plates were incubated at room temperature in the dark for 3 min and read using a Spark Cyto plate reader (Tecan Group Ltd., Männedorf, Switzerland). The assay protocol included orbital shaking for 3 min (1 mm amplitude), followed by luminescence acquisition with a 200 ms settle time and 500 ms integration time, using OD2 attenuation mode. Luminescence values were recorded as raw counts per second. For each mRNA sample, technical replicates were median-collapsed, and data were visualized using R (v4.4.2) and the ggplot2 package (v3.5.1)[29].

3. Results and Discussion

3.1. Reduction of high-molecular-weight impurities (HMWI)

Previous studies have shown that precipitation can reduce aggregates and HMWI by up to 86 %. However, despite this reduction, aggregates can still make up as much as 20 % of the total mRNA content [29]. These impurities often result from the intrinsic properties of mRNA, which, as a single-stranded molecule, can fold into secondary structures such as hairpins and loops or associate with other mRNA strands to form larger aggregates. Despite their potential impact, mRNA aggregates are not explicitly mentioned in the publicly available specifications for COVID-19 vaccines. This highlights the need for a deeper understanding and characterization of oligonucleotide aggregation. Such species can compromise mRNA stability and function, ultimately reducing the therapeutic potential of the final product. Therefore, efficient removal of HMWI is essential to achieving the required levels of purity, stability, and product consistency [31]. Studies have demonstrated that a heating step can significantly reduce mRNA aggregates [31–33]. To investigate its feasibility in a continuous process, the temperature and incubation time were evaluated for their impact on HMWI reduction. Additionally, the effects of pH and buffer composition on HMWI formation were evaluated.

Fluc and Covid mRNA were precipitated under different buffer and pH conditions (100 mM citrate buffer pH 4, 100 mM sodium citrate buffer pH 5.6, 100 mM MES buffer pH 7, 100 mM Tris buffer pH 8 and pH 9) to assess the impact of pH and buffer species on HMWI content **(**Fig. 1**)**. For Fluc mRNA **(**Fig. 1**A)**, HMWI levels were consistently lowest at pH 4, indicating that acidic conditions may effectively suppress impurity formation. In contrast, at neutral and alkaline pH values (pH 7–9), HMWI content was slightly elevated and showed minimal variation with increasing concentrations of PEG6000. Notably, the highest levels of HMWIs were observed at pH 5.6, highlighting a distinct pH-dependent effect and suggesting that this intermediate acidity may promote impurity formation under the tested conditions. Covid mRNA **(**Fig. 1**B)** showed a more stable HMWI content across the different pH conditions, with less pronounced variation compared to Fluc mRNA. As observed with Fluc, HMWI levels were slightly higher at neutral and alkaline pH values (pH 7–9). However, no increase in HMWI content was detected at pH 5.6, in contrast to the trend seen with Fluc mRNA. In both mRNA types, HMWI levels remained relatively unchanged with increasing PEG6000 concentrations, these findings, as shown previously [29],

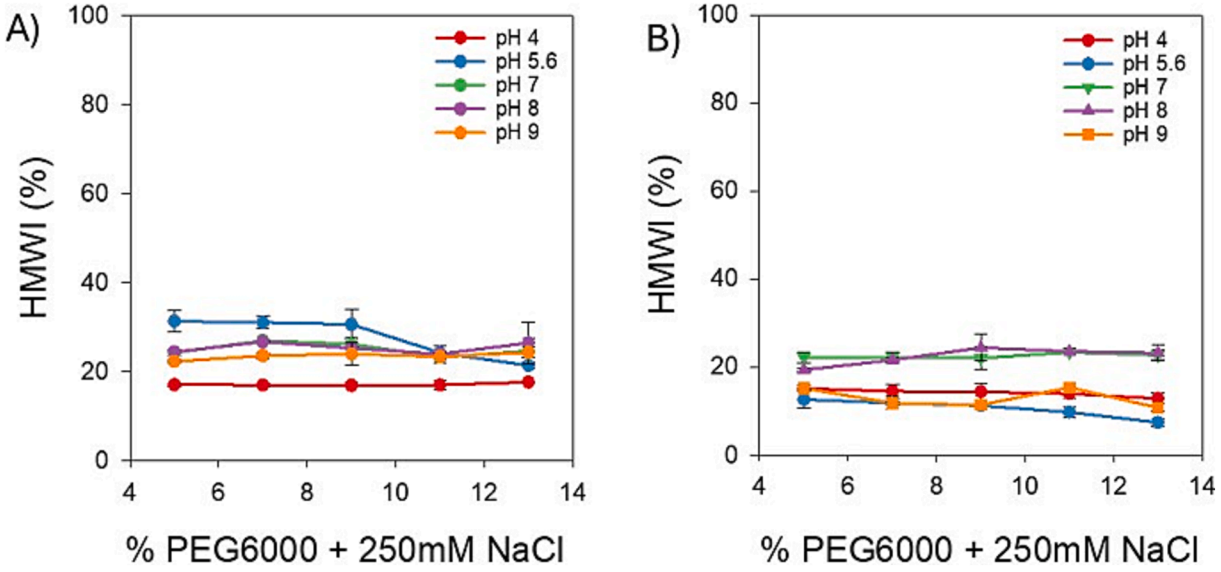

Fig. 1. Screening for A) Fluc and B) Covid for different pH values. Each sample was analyzed three times, and the data are reported as the average value with the corresponding standard deviation.

suggest that the precipitation process does not induce aggregate formation and that HMWI content is primarily influenced by pH and buffer species rather than by precipitation. This pH-dependent behavior is consistent with previous studies showing that both buffer species and pH significantly impact mRNA degradation and stability [34]. For instance, Bauer et al. [35] demonstrated that hydrolysis rates increase as pH decreases, and mRNA is generally more stable in weakly alkaline environments (pH 7–8), a principle reflected in the formulation of approved Moderna and Pfizer/BioNTech COVID-19 RNA vaccines. However, Mounir et al. [36] reported that in the presence of specific buffering agents, such as sodium citrate and Tris-HCl, RNA hydrolysis can be catalyzed by Mg^{2+} in a pH-dependent manner. This may explain the elevated HMWI levels observed for Fluc mRNA at pH 5.6, where sodium citrate was used as the buffer. Moreover, mRNA degradation was independent of buffer concentration [37]. Additionally, no significant impact was observed on mRNA purity, precipitation efficiency, or recovery yields across the tested conditions, nor was there any notable reduction in HMWI levels. Recovery yields for the selected precipitation conditions were extensively evaluated and reported previously [29]. These findings highlight the importance of careful pH and buffer selection to minimize HMWI formation during mRNA purification processes.

Afterwards, Fluc (Fig. 2**A)** and Covid mRNA (Fig. 2**B)** were incubated at varying temperatures (40 °C, 50 °C, 60 °C, and 70 °C) for 2, 5, and 10 min to assess the impact of heat on HMWI reduction. The results reveal that higher temperatures accelerate the reduction of HMWI over time. At 40 °C, HMWI reduction occurs at a slower rate compared to elevated temperatures, suggesting that lower temperatures are less effective in clearing these impurities. Conversely, at 70 °C, HMWI levels rapidly decrease and stabilize at lower percentages, demonstrating a more efficient clearance of high-molecular-weight species. HMWI reduction occurs within the first few minutes, indicating that extended heating would not provide additional benefits and could potentially lead to mRNA degradation. Therefore, a 2 min treatment is sufficient to achieve optimal HMWI reduction. This process effectively targets non-covalent aggregates, which are vulnerable to thermal disruption [31–33]. However, it has been observed that covalent aggregates are heat-resistant and cannot be removed through this method. These

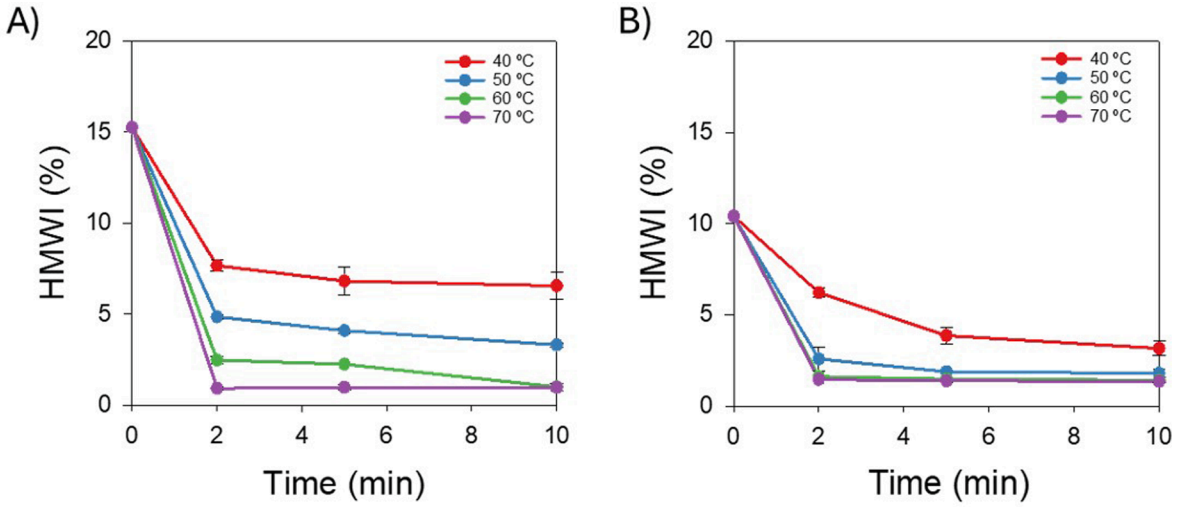

Fig. 2. High molecular weight impurities content (%) as a function of time under different temperature conditions (40 °C, 50 °C, 60 °C, and 70 °C) for a) Fluc and b) Covid mRNA. Each sample was analysed three times, and the data are reported as the average value with the corresponding standard deviation.

findings are significant for mRNA purification, where controlling aggregate formation is crucial for maintaining product purity. Importantly, no mRNA degradation was observed, suggesting that the thermal treatment selectively reduces high-molecular-weight impurities without compromising mRNA integrity. Additionally, aggregates did not reform upon cooling.

3.2. Optimization of concentration and washing factors for mRNA purification

To improve the efficiency of sequential filtration, the balance between concentration and washing steps needs to be optimized to maximize impurity clearance while minimizing buffer consumption. The effect of concentration and washing factors on mRNA and LMWI content were evaluated **(**Fig. 3**).**

Precipitated mRNA was fed at a constant flow rate from a tank into a hollow fiber membrane, with a controlled permeate flow rate to prevent uncontrolled membrane fouling. During concentration experiments, the volume was reduced to a predetermined level, achieving concentration factors of 2 and 3 **(**Fig. 3**).** For the washing steps, the mRNA slurry was diluted with a defined amount of washing solution at dilution factors of 2, 4, 6 and 10 until the initial volume was reestablished. After each stage, the collected and concentrated mRNA precipitate slurry was diluted 1:10 with RNAse free water and subsequently analyzed by SEC to assess purity and yield.

Concentration experiments **(**Fig. 3**A)** showed a slight increase in mRNA content but no significant reduction in LMWI. With increasing concentration factors (×2 and ×3), LMWI remained the predominant fraction, indicating that concentration alone is ineffective for impurity removal. Further concentration led to product losses without additional purification benefit. Recent studies have shown that alternative filters can enhance mRNA concentration [38,39]. However, these filters generally present large membrane areas, which are not suitable for the scope of this work. However, further optimization of mRNA concentration processes may still be feasible. Nonetheless, technical challenges must be considered, as current IVT yields ranging from 0.5 to 24 g/L [40–42], can complicate downstream purification strategies particularly when working with high concentration. The increased viscosity of the samples will further complicate the filtration process. In contrast, the washing factor study **(**Fig. 3**B)** showed a clear, progressive reduction in LMWI content as the washing factor increased. After a washing factor of 6 the purity did not increase further compared to a washing factor of 10 reaching the highest purity level (~80 %). These results confirm that washing is a highly effective step in impurity removal. Therefore, we selected a minimum washing factor of 6 for further experiments, since concentration resulted in product loss.

3.3. Critical flux and filtration module determination

Determining the critical flux is crucial for assessing continuous membrane filtration performance and optimizing process conditions. It helps compare different membrane modules and select the most efficient one for a given application. The critical flux marks the point where filtration shifts from stable operation to increased fouling, causing a rapid decline in permeate flux. In continuous processes, where long-term stability is critical, operating below the critical flux ensures consistent performance, reduced fouling, and extended membrane lifespan [30].

Critical flux was determined with different membranes to select the hollow fiber membrane require which one was more suitable for the process in terms of product and process conditions. Two main membrane types were evaluated polyethersulfone (PES) and mixed cellulose ester (ME) **(**Fig. 4**).** Results show a significant increase of the TMP when using the ME membrane indicating a fast fouling of the membrane at already 21 LMH and therefore it cannot be used for long-term operations. On the contrary PES membrane could be operated to much higher fluxes, with a critical flux of 138 LMH. Subsequently, the effect of fiber internal diameter was assessed for PES membranes with either a 1 mm or 0.5 mm internal diameter. The results also indicate improved performance when operating with a 1 mm fiber internal diameter compared to 0.5 mm where almost immediate fouling was observed. Consequently, PES membranes with a 1 mm fiber internal diameter were selected for continuous solid–liquid separation **(**Fig. 4**).** Subsequently, the critical flux was evaluated under the operating conditions representative of the 1st and 2nd stages of the continuous TFF process, using Fluc mRNA in buffer 1 (13 % PEG6000 and 250 mM NaCl), previously determined in Pons Royo et al. [29] and buffer 2 (750 mM NaAc). For PES membranes using buffer 1, the critical flux was determined to be 138 LMH, while for the second TFF stage with buffer 2, no fouling was observed during the experiment. However, for consistency flux was set to 231 LMH. The

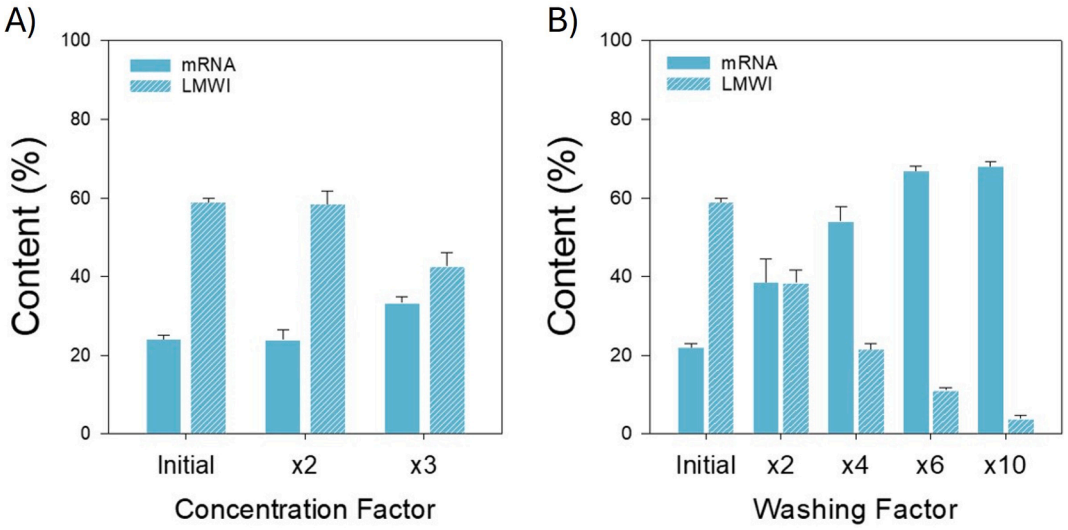

Fig. 3. Effect of concentration and washing factors on the content of mRNA and LMWI (%). Left: Concentration performance at different concentration factors (x2 and x3) compared to the initial condition. Right: Washing efficiency at increasing washing factors (x1 to x10). Each sample was analysed three times, and the data are reported as the average value with the corresponding standard deviation.

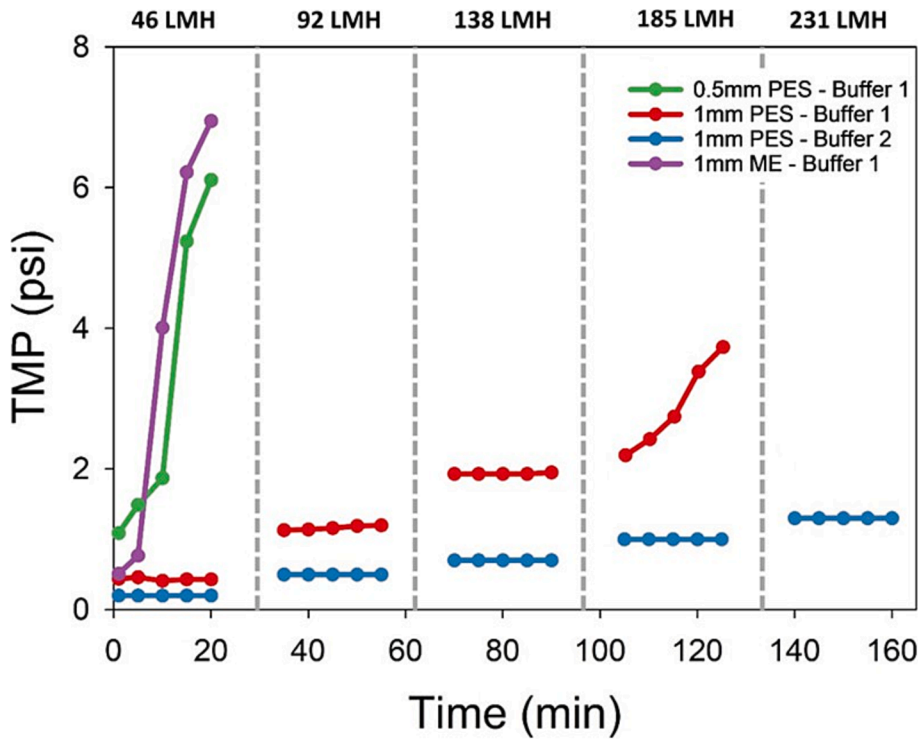

Fig. 4. Critical flux experiments were conducted in recycle mode using process-relevant mRNA concentrations in buffer 1 (13 % PEG 6000 and 250 mM NaCl) and buffer 2 (750 mM NaAc, pH 5.5). Membrane material, module internal diameter, experimental conditions, and maximum critical flux (LMH) are provided in the figure legend.

selection of the hollow fiber membranes was based on their commercial availability.

3.4. *Continuous precipitation and filtration*

A flow diagram of the complete system is presented (Fig. 5), which consists of a self-assembled tubular reactor, two hollow fiber membranes, and a final redissolution step using a water bath. Due to the limited amount of material available, we were only able to conduct two 1-hour runs to assess the continuous process. The 1-hour runs were sufficient to demonstrate the stability and feasibility of the continuous process within the given timeframe. During a single 1-hour run, 60 mg of mRNA were processed, which corresponds to more than 2,000 doses of mRNA vaccine [43].

The IVT crude and the precipitating solution (PEG6000 with NaCl) were mixed at a controlled ratio by adjusting their respective flow rates to achieve a final precipitation condition of 13 % PEG6000 and 250 mM NaCl. Precipitation was carried out in a custom-assembled tubular

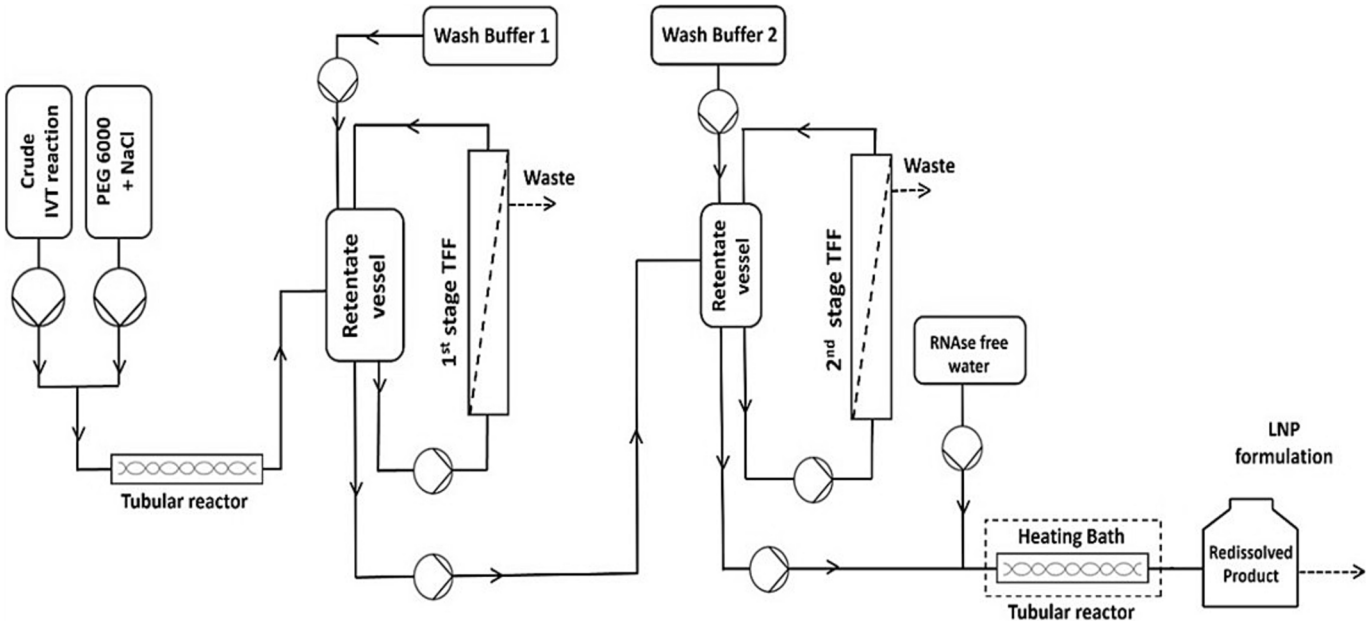

Fig. 5. Schematic representation of the fully continuous mRNA purification process.

reactor equipped with helical static mixers to ensure efficient mixing and prevent precipitate settling. The residence time of the tubular reactor was determined by the length, diameter and the applied flow rate, resulting in a residence time of 20 min, previously determined in Pons Royo et al. [29]. Following precipitation, the precipitate was fed into the first retention vessel, washed with 20 % PEG6000 and 250 mM NaCl, and then pumped into the first TFF stage. Here, the precipitate was washed by a factor of 5 (ratio of feed flow to bleed flow) using tangential microfiltration (0.2 μm pore size; 13 cm^2 membrane area). The precipitate stream over the membrane was pumped at a theoretical feed flux of 2308 LMH. To accelerate equilibration to a steady state, the bleed flow was closed for 8 min before being reopened and fed into the second retention vessel for the next TFF stage (0.2 μm pore size; 13 cm^2 membrane area). The time required to achieve steady state was estimated using a numerically solved mass balance model. In the second TFF stage, the precipitate was washed with 750 mM NaAc, was washed by a factor of 6 using tangential microfiltration (0.2 μm pore size; 13 cm^2 membrane area). The precipitate stream over the membrane was again operated at a theoretical feed flux of 2308 LMH. As in the first stage, the bleed was temporarily closed for 5 min to establish steady-state conditions. After the 2nd TFF, the precipitate was diluted 1:10 with RNAse-free water to reach an mRNA concentration of ~ 60 μg/mL for LNP encapsulation and a final buffer concentration of 35 mM NaAc [44–46]. The stream was then pumped into a water bath at 70 °C through a tubular reactor with 2 min residence to dissolve the mRNA and remove aggregates.

Afterwards, mRNA samples were taken and analyzed for purity and yield by SEC (Fig. 6). The final product exhibited consistent purity and yield across both runs, mRNA concentration remained stable at 60 μg/mL throughout the process, meeting LNP encapsulation requirements (Fig. 6**A**). The continuous process achieved yields of 88 % and 92 %, as determined by mass balance calculations (Fig. 6**B**). Membrane retention accounted for 8–12 % of total mRNA loss after rinsing with RNase-free water. Purity remained consistently high at 95 %, with a significant reduction in HMWI from 46 % to 0.6 %, and low molecular weight impurities LMWI from 40 % to 4 % (Fig. 6**B**). Additionally, analysis confirmed the integrity of the mRNA, with no signs of fragmentation, degradation, or dsRNA formation. HMWI did not re-form after the system was cooled down. Residual pDNA was not quantified for the precipitated, purified FLuc sample, as the initial concentration provided by the manufacturer was already below the threshold specified by regulatory guidelines. Additionally, the integrity and activity of the purified, precipitated mRNA were evaluated through in vitro protein expression experiments. The Fluc expression levels obtained were similar to those achieved with commercially purified Fluc and chromatography-purified samples (from the industrial partner or commercially available positive controls), demonstrating that precipitation does not compromise mRNA functionality (Fig. 7).

Key process parameters, such as TMP (Fig. 8), were continuously monitored. The results demonstrated minimal fluctuations over time, with TMP remaining stable throughout the run, showing a gradient of < 0.5 psi/h for TFF1 and < 0.3 psi/h for TFF2. This stability suggests strong potential for long-term continuous operation (Fig. 8) while confirming minimal fouling. Moreover, both filters followed a consistent trend across runs, further reinforcing the robustness of the process.

The precipitation method outperformed the Oligo-DT chromatography approach for mRNA purification in both purity and yield (Table 1). Precipitation achieved a purity of around 95 %, while chromatography-based purification reached only 82 %. Both methods resulted in similar levels of residual LMWI, with precipitation achieving slightly lower impurity levels at 4 %, compared to 8 % in the chromatography-based product. For HMWI, the precipitation process demonstrated better performance, reducing the concentration to 0.6 %, while chromatography resulted in a higher residual HMWI content of

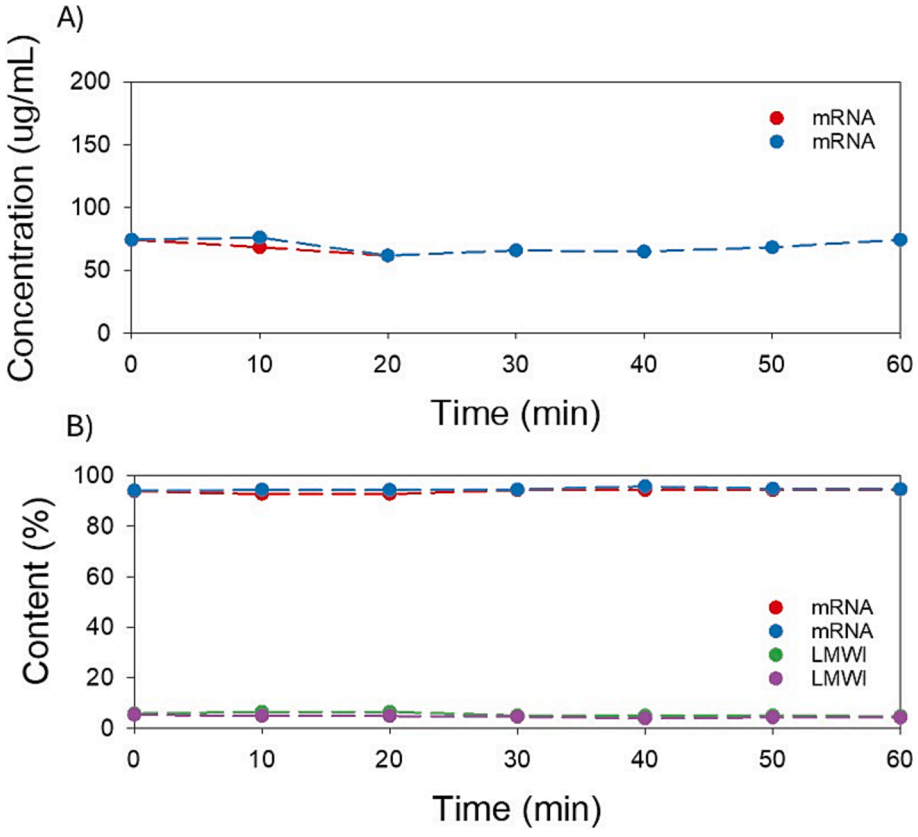

Fig. 6. A) Time-course profile of mRNA concentration during a continuous purification run over 60 min. B) Corresponding percentage profiles of LMWI and mRNA content over time.

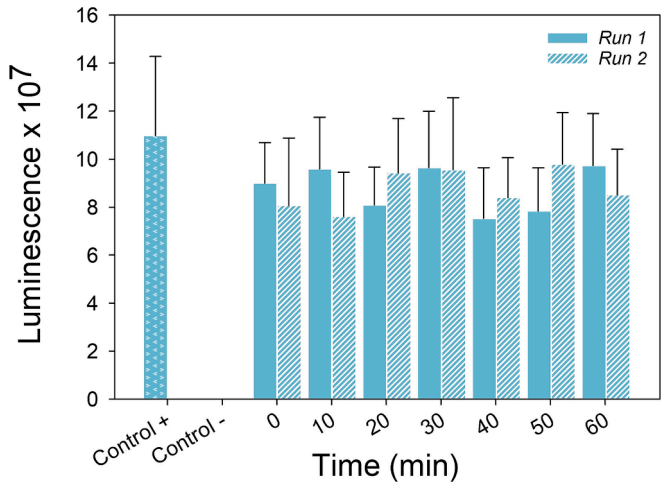

Fig. 7. Luminescence measurements over time for the two independent experimental runs. Positive (Control +) and negative (Control −) controls were included for comparison. Each sample was measured three times (n = 3), and error bars represent standard deviations.

12 %. In terms of yield, the precipitation-based process achieved approximately 90 %, while Oligo-DT purification typically yields between 86 % and 93 %. However, the additional pre-treatment steps required for chromatography, such as buffer exchange and heat treatment, are likely to result in a lower overall yield compared to the precipitation method.

Furthermore, the precipitation process offers several advantages over conventional methods, such as Oligo-DT chromatography purification. First, precipitation operates independently of solute concentration, so the quantity of precipitant needed is determined by the total volume of the solution rather than the mRNA concentration in the input stream. Consequently, no further pretreatments are required for the purification as it would be required for filters or chromatography systems at high concentration. Precipitation can be performed without interrupting the mass flow within units in a fully continuous mode. Unlike chromatography, which requires cyclic operation or countercurrent loading, continuous precipitation can be integrated seamlessly with upstream and downstream steps, eliminating the need for intermediate surge tanks. It can also be integrated into the existing manufacturing process for mRNA-based products without significant complexity. At an industrial scale, the goal of an IVT (in vitro transcription) reaction is to achieve a production rate of up to 40 g per day. In a continuous setup that would correspond to a flow of 5 mL/min at concentrations up to 8 g/L. To process such feeds, the process can be easily scaled up by increasing the size of tubular reactors, where the flow rate grows proportionally to the square of the reactor's internal diameter [47,48] (Table 2). Therefore, the tubular reactor must increase the cross-sectional area up to 10 mm. The required filter area can be estimated by comparing the flow rate to the filtration flux. To maintain performance under the new conditions, the filter area should be scaled proportionally by increasing the total membrane surface area. Based on current operation, the filter area should be increased to approximately 170–350 cm^2 [49]. However, further experiments should be performed to evaluate the required filter area for higher concentrations. The required flows for LNP formulation and final concentration of mRNA in a specific buffer by simple dilution and it can be efficiently coupled between unit operations, eliminating the need for further purification steps or buffer exchange. Furthermore, adapting continuous precipitation to GMP manufacturing would be straightforward, as the required tubing and filters are readily available as fully sterilized, single-use materials from various suppliers. Additionally, the equipment volumes required are significantly smaller compared to those needed for the current downstream processes, which would consequently reduce manufacturing costs, including the need for reduced GMP space.

4. Conclusion

A fully continuous precipitation-based process for mRNA purification was presented. mRNA was continuously precipitated from the crude in vitro transcription mixture, followed by two sequential microfiltration steps. The first step was used for washing, while the second removed the precipitant and buffer exchange, allowing for direct encapsulation into LNPs. The process achieved higher yields and purity levels compared to traditional chromatography-based purification methods. In contrast to semi-continuous chromatography systems that operate in cycles, this approach was operated fully in continuous.

Table 1
Comparison of chromatography- and precipitation-based mRNA purification, and suggested quality attributes and process parameters for mRNA-based products [29].

Quality attribute/ Process parameter	Suggested acceptance criteria	Oligo-dT purified construct − Fluc	Precipitated purified − Fluc
Recovery yield	97–70 %	n.d.	92 %
Purity	–	93 %	95 %
Fragment purity	90 %	93 %	90 %
Residual pDNA	< 1 %	< 1 %‡	n.d.
Residual enzymes	<5.0 µg/mL	1.96 ug/mL†	b.d.l.
dsRNA content	< 1 %	< 1 % *	0.11 %

Values marked with * were reported by the industrial partner and determined using dot blot analysis;
† values were measured using the NanoOrange assay; and ‡ values were obtained by qPCR.
N.d. corresponds to not determined; B.d.l. indicates below detection limit.

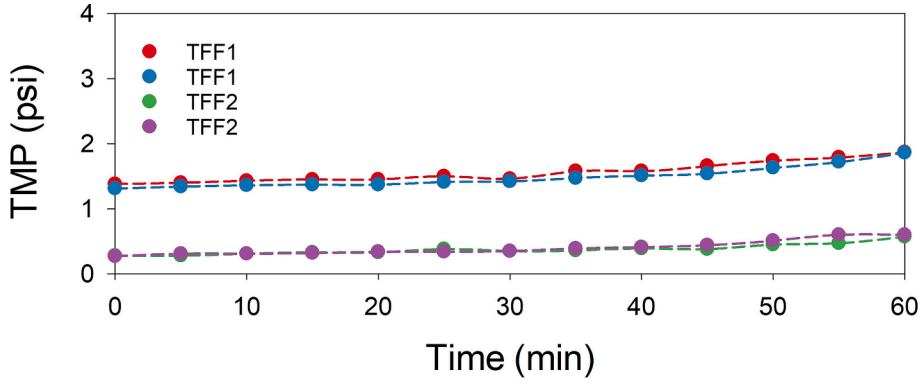

Fig. 8. Transmembrane pressure (TMP) profiles during continuous mRNA purification runs over 60 min.

Table 2
Scale up and integration scenario from laboratory to full industrial scale.

Operation	In vitro reaction		Continuous precipitation		LNP formulation	
Scale	Laboratory	Industrial	Laboratory	Industrial	Laboratory	Industrial
Flow (mL/min)	0.1–0.5	5	0.5–2	5	20–50	200–500
Concentration mRNA (g/L)	1–5	5–8	1–3.5	5–8	100–50 μg/L	100–50 μg/L
Cross sectional area – Tubular reactor (mm^2)	–	–	3.20	10	–	–
Filter membrane (cm^2)	–	–	13	~ 170—350	–	–

Moreover, the process has demonstrated robustness and reproducibility, ensuring consistent and reliable performance over the full run, reducing costs and space. The process can be easily coupled with IVT reaction and to LNP encapsulation without any other requirements. Furthermore, no degradation, aggregation, or impact on LNP encapsulation was observed, making it suitable for large-scale purification applications.

CRediT authorship contribution statement

Maria del Carme Pons Royo: Writing – original draft, Validation, Supervision, Methodology, Investigation, Formal analysis, Data curation, Conceptualization. **Tyler Arnold:** Investigation. **Isabella Perez Rodriguez:** Investigation. **Nicole Ostrovsky:** Investigation. **Mushriq Al-Jazrawe:** Investigation. **Andrew Hatas:** Writing – review & editing, Methodology, Investigation. **Allan S. Myerson:** Writing – review & editing, Supervision, Funding acquisition, Conceptualization. **Richard D. Braatz:** Writing – review & editing, Supervision, Funding acquisition, Conceptualization.

Declaration of competing interest

The authors declare that they have no known competing financial interests or personal relationships that could have appeared to influence the work reported in this paper.

Acknowledgements

We thank the Koch Institute's Robert A. Swanson (1969) Biotechnology Center for technical support, specifically the Massachusetts Institute of Technology Koch Institute High Throughput Sciences Core Facility (RRID:SCR_026340).

This research was supported by the U.S. Food and Drug Administration under the FDA BAA-22-00123 program, Award Number 75F40122C00200.

Data availability

Data will be made available on request.

References

[1] J.R. Mascola, A.S. Fauci, *Novel vaccine technologies for the 21st century*, Nat. Rev. Immunol. 20 (2) (2020) 87–88.
[2] M. Li, et al., *COVID-19 vaccine development: milestones, lessons and prospects*, Signal Transduct. Target. Ther. 7 (1) (2022) 146.
[3] Y.-S. Wang, et al., *mRNA-based vaccines and therapeutics: an in-depth survey of current and upcoming clinical applications*, J. Biomed. Sci. 30 (1) (2023) 84.
[4] J. Whitley, et al., *Development of mRNA manufacturing for vaccines and therapeutics: mRNA platform requirements and development of a scalable production process to support early phase clinical trials*, Transl. Res. 242 (2022) 38–55.
[5] S. Daniel, et al., *Quality by Design for enabling RNA platform production processes*, Trends Biotechnol. 40 (10) (2022) 1213–1228.
[6] S.S. Rosa, et al., *mRNA vaccines manufacturing: challenges and bottlenecks*, Vaccine 39 (16) (2021) 2190–2200.
[7] R. Miklavčič, et al., *High Recovery Chromatographic Purification of mRNA at Room Temperature and Neutral pH*, Int. J. Mol. Sci. 24 (18) (2023) 14267.
[8] A. Kanavarioti, *HPLC methods for purity evaluation of man-made single-stranded RNAs*, Sci. Rep. 9 (1) (2019) 1019.
[9] P. Gagnon, *Purification of nucleic acids : ǂa ǂhandbook for purifying plasmid DNA and mRNA for gene therapy and vaccines*, Ajdovščina, BIA Separations, 2020.
[10] D. Weissman, et al., *HPLC Purification of In Vitro Transcribed Long RNA*, in: P. M. Rabinovich (Ed.), *Synthetic Messenger RNA and Cell Metabolism Modulation: Methods and Protocols*, Humana Press, Totowa, NJ, 2013, pp. 43–54.
[11] K. Karikó, et al., *Generating the optimal mRNA for therapy: HPLC purification eliminates immune activation and improves translation of nucleoside-modified, protein-encoding mRNA*, Nucleic Acids Res. 39 (21) (2011) e142–e.
[12] P. Gagnon, et al., *Two new capture options for improved purification of large mRNA*, Cell and Gene Therapy Insights 6 (2020) 1035–1046.
[13] Afeyan, W.J.I.L.B.G.A.B., *Ion exchange purification of mrna*. 2014.
[14] S.S. Rosa, et al., *Exploring Bayesian methods in chromatographic development: increasing the capacity of the mRNA affinity ligand*, Sep. Purif. Technol. 367 (2025) 132881.
[15] E.A. Dewar, et al., *Improved mRNA affinity chromatography binding capacity and throughput using an oligo-dT immobilized electrospun polymer nanofiber adsorbent*, J. Chromatogr. A 1717 (2024) 464670.
[16] N. Mencin, et al., *Development and Scale-up of Oligo-Dt Monolithic Chromatographic Column for Mrna Capture through Understanding of Base-Pairing Interactions*, SSRN Electron. J. (2022).
[17] M. Korenč, et al., *Chromatographic purification with CIMmultus™ Oligo dT increases mRNA stability*, Cell and Gene Therapy Insights 7 (2021) 1207–1216.
[18] S. Fekete, et al., *Salt gradient and ion-pair mediated anion exchange of intact messenger ribonucleic acids*, Journal of Chromatography Open 2 (2022) 100031.
[19] G. Recanati, et al., *Integration of a perfusion reactor and continuous precipitation in an entirely membrane-based process for antibody capture*, Eng. Life Sci. 23 (10) (2023) e2300219.
[20] M.d.C. Pons Royo, T. De Santis, D. Komuczki, P. Satzer, A. Jungbauer, Continuous precipitation of antibodies by feeding of solid polyethylene glycol, Sep. Purif. Technol. 304 (2023) 122373, https://doi.org/10.1016/j.seppur.2022.122373.
[21] Y. Zhu, et al., *Towards platformization of monoclonal antibody capture precipitation solution conditions in the PEG-zinc precipitant system*, Sep. Purif. Technol. 361 (2025) 131138.
[22] N. Hammerschmidt, S. Hobiger, A. Jungbauer, *Continuous polyethylene glycol precipitation of recombinant antibodies: Sequential precipitation and resolubilization*, Process Biochem. 51 (2) (2016) 325–332.
[23] D. Burgstaller, A. Jungbauer, P. Satzer, *Continuous integrated antibody precipitation with two-stage tangential flow microfiltration enables constant mass flow*, Biotechnol. Bioeng. 116 (5) (2019) 1053–1065.
[24] M.d.C. Pons Royo, A. Jungbauer, Polyethylene glycol precipitation: Fundamentals and recent advances, Prep. Biochem. Biotechnol. 55 (8) (2025) 935–954, https://doi.org/10.1080/10826068.2025.2470220.
[25] M. Minervini, et al., *Continuous precipitation-filtration process for initial capture of a monoclonal antibody product using a four-stage countercurrent hollow fiber membrane washing step*, Biotechnol. Bioeng. 121 (8) (2024) 2258–2268.
[26] M. Minervini, et al., *Optimizing particle morphology during antibody precipitation for enhanced tangential flow filtration performance*, Sep. Purif. Technol. 338 (2024) 126574.
[27] Matthew R. Mergy, M.A.G.-D., Yuncan Zhu, Mirko Minervini, Ali Behboudi, Steven M. Cramer, Todd M. Przybycien, and Andrew L. Zydney,, *Demonstration of an integrated and continuous monoclonal antibody purification process with capture via precipitation*, in *Integrated Continuous Biomanufacturing VI, ECI Symposium Series*. 2024.
[28] X. Feng, et al., *Rapid and high recovery isolation of mRNA from in vitro transcription system by ammonium sulphate precipitation at room temperature*, Sep. Purif. Technol. 336 (2024) 126331.
[29] M.D.C. Pons Royo, et al., *Purification of messenger RNA directly from crude IVT using polyethylene glycol and NaCl precipitation*, Process Biochem. 156 (2025) 263–273.
[30] Z. Li, A.L. Zydney, *Effect of zinc chloride and PEG concentrations on the critical flux during tangential flow microfiltration of BSA precipitates*, Biotechnol. Prog. 33 (6) (2017) 1561–1567.
[31] A. Goyon, et al., *Separation of Plasmid DNA Topological Forms, Messenger RNA, and Lipid Nanoparticle Aggregates using an Ultrawide Pore size Exclusion Chromatography Column*, Anal. Chem. 95 (40) (2023) 15017–15024.
[32] J. Camperi, et al., *Comprehensive Impurity Profiling of mRNA: evaluating Current Technologies and Advanced Analytical Techniques*, Anal. Chem. 96 (9) (2024) 3886–3897.
[33] J. Camperi, et al., *Physicochemical and Functional Characterization of Differential CRISPR-Cas9 Ribonucleoprotein Complexes*, Anal. Chem. 94 (2) (2022) 1432–1440.
[34] F. Cheng, et al., *Research advances on the Stability of mRNA Vaccines*, Viruses 15 (3) (2023).
[35] T. Bauer, et al., *Effect of food components and processing parameters on DNA degradation in food*, Environ. Biosaf. Res. 3 (4) (2004) 215–223.

[36] M.G. Abouhaidar, I.G. Ivanov, *Non-Enzymatic RNA Hydrolysis Promoted by the combined Catalytic activity of Buffers and Magnesium Ions*, Zeitschrift Für Naturforschung C 54 (7–8) (1999) 542–548.
[37] U. Chheda, et al., *Factors Affecting Stability of RNA – Temperature, Length, Concentration, pH, and Buffering Species*, J. Pharm. Sci. 113 (2) (2024) 377–385.
[38] A. Javidanbardan, et al., *Single-pass tangential flow filtration (SPTFF) for continuous mRNA concentration and purification*, J. Membr. Sci. 719 (2025) 123730.
[39] A. Behboudi, et al., *Vibration-assisted ultrafiltration dramatically improves mRNA purification*, Sep. Purif. Technol. 363 (2025) 132179.
[40] Y. Sari, et al., *Comprehensive evaluation of T7 promoter for enhanced yield and quality in mRNA production*, Sci. Rep. 14 (1) (2024) 9655.
[41] D. Pregeljc, et al., *Increasing yield of in vitro transcription reaction with at-line high pressure liquid chromatography monitoring*, Biotechnol. Bioeng. 120 (3) (2023) 737–747.
[42] J. Boman, et al., *Quality by design approach to improve quality and decrease cost of in vitro transcription of mRNA using design of experiments*, Biotechnol. Bioeng. 121 (11) (2024) 3415–3427.
[43] E.D. Moreira, et al., *Safety and Efficacy of a Third Dose of BNT162b2 Covid-19 Vaccine*, N. Engl. J. Med. 386 (20) (2022) 1910–1921.
[44] A. Lamoot, et al., *Successful batch and continuous lyophilization of mRNA LNP formulations depend on cryoprotectants and ionizable lipids*, Biomater. Sci. 11 (12) (2023) 4327–4334.
[45] S.J. Shepherd, et al., *Throughput-scalable manufacturing of SARS-CoV-2 mRNA lipid nanoparticle vaccines*, Proc. Natl. Acad. Sci. 120 (33) (2023) e2303567120.
[46] S. Li, et al., *Payload distribution and capacity of mRNA lipid nanoparticles*, Nat. Commun. 13 (1) (2022) 5561.
[47] N. Lingg, et al., *Continuous cold ethanol precipitation of immunoglobulin G from human plasma*, Process Biochem. 132 (2023) 121–129.
[48] Buglioni, L., et al., *Technological Innovations in Photochemistry for Organic Synthesis: Flow Chemistry, High-Throughput Experimentation, Scale-up, and Photoelectrochemistry*. Chemical reviews, 2021. **XXXX**.
[49] Lutz, H., *Ultrafiltration for Bioprocessing*. 2015: Woodhead Publishing.